Title: Disruption of Aldehyde Dehydrogenase 2 protects against bacterial infection

Authors: Samuel B. Berry[1], Scott Espich[2], Nguyen T.T. Thuong[3,4], Xuling Chang[5,6,7], Rajkumar Dorajoo[6,8], Chiea-Chuen Khor[8,9], Chew-Kiat Heng[6,7], Jian-Min Yuan[10], Douglas Fox[1], Andrea Anaya-Sanchez[11], Logan Tenney[12],Christopher J. Chang[12,13], Dmitri I. Kotov[1,14], Russell E. Vance[1,14], Sarah J. Dunstan[5], K. Heran Darwin[15]*, Sarah A. Stanley[1,2]*

*These authors contributed equally to this work

Affiliations:

1. Division of Immunology and Pathogenesis, Department of Molecular and Cell Biology, University of California, Berkeley, Berkeley, CA 94720
2. Division of Infectious Disease and Vaccinology, School of Public Health, University of California, Berkeley, Berkeley, CA 94720
3. Oxford University Clinical Research Unit, Ho Chi Minh City, Vietnam
4. Nuffield Department of Medicine, University of Oxford, Oxford, United Kingdom
5. Department of Infectious Diseases, Peter Doherty Institute for Infection and Immunity, University of Melbourne, Melbourne, Australia
6. Department of Paediatrics, Yong Loo Lin School of Medicine, National University of Singapore and National University Health System, Singapore 119228, Singapore.
7. Khoo Teck Puat - National University Children's Medical Institute, National University Health System, Singapore, 119074, Singapore
8. Genome Institute of Singapore (GIS), Agency for Science, Technology and Research (A*STAR), 60 Biopolis Street, Genome, Singapore 138672, Republic of Singapore
9. Singapore Eye Research Institute, Singapore National Eye Centre, Singapore, 169856, Singapore
10. Division of Cancer Control and Population Sciences, UPMC Hillman Cancer Center, University of Pittsburgh, Pittsburgh, PA, 15232, USA.
Department of Epidemiology, School of Public Health, University of Pittsburgh, Pittsburgh, PA, 15261, USA
11. Graduate Group in Microbiology, University of California, Berkeley, Berkeley, CA 94720
12. Department of Chemistry, University of California, Berkeley, CA 94720
13. Division of Molecular Therapeutics, Department of Molecular and Cell Biology, University of California, Berkeley, CA 94720
14. Howard Hughes Medical Institute, University of California, Berkeley
15. Department of Microbiology, New York University Grossman School of Medicine, New York, NY 10016.

Contact: sastanley@berkeley.edu, heran.darwin@med.nyu.edu

One sentence summary: Aldehydes produced by host cells contribute to the control of bacterial infections.

Abstract: The *ALDH2*2* (rs671) allele is one of the most common genetic mutations in humans, yet the positive evolutionary selective pressure to maintain this mutation is unknown, despite its association with adverse health outcomes. ALDH2 is responsible for the detoxification of metabolically produced aldehydes, including lipid-peroxidation end products derived from inflammation. Here, we demonstrate that host-derived aldehydes 4-hydroxynonenal (4HNE), malondialdehyde (MDA), and formaldehyde (FA), all of which are metabolized by ALDH2, are directly toxic to the bacterial pathogens *Mycobacterium tuberculosis* and *Francisella tularensis* at physiological levels. We find that *Aldh2* expression in macrophages is decreased upon immune stimulation, and that bone marrow-derived macrophages from *Aldh2*$^{-/-}$ mice contain elevated aldehydes relative to wild-type mice. Macrophages deficient for *Aldh2* exhibited enhanced control of *Francisella* infection. *Finally,* mice lacking *Aldh2* demonstrated increased resistance to pulmonary infection by *M. tuberculosis*, including in a hypersusceptible model of tuberculosis, and were also resistant to *Francisella* infection. We hypothesize that the absence of ALDH2 contributes to the host's ability to control infection by pathogens such as *M. tuberculosis* and *F. tularensis*, and that host-derived aldehydes act as antimicrobial factors during intracellular bacterial infections.

Main Text: Loss-of-function mutations in aldehyde dehydrogenase 2 (*ALDH2*) are highly prevalent, affecting up to 500 million individuals of East Asian descent (*1*). The most common mutant allele, *ALDH2*2* (rs671), encodes an s E487K mutation that results in a dominant-negative form of the enzyme (*2*). ALDH2 is notably required for converting acetaldehyde, a toxic intermediate of ethanol metabolism, into acetate, but its primary function is to detoxify metabolically produced aldehydes. Hetero- or homozygous carriers of *ALDH2*2* experience adverse physiological effects upon consumption of alcohol due to an accumulation of acetaldehyde (*3*). Even in the absence of alcohol consumption, loss of ALDH2 function is associated with an increased risk of cancer, heart disease, and neurological disorders (*4*, *5*).

The selective pressure that has maintained *ALDH2*2* in the human population, despite its detrimental effects on human health, remains unknown. The *ALDH2*2* allele was reported to be associated with a decreased risk of active tuberculosis (TB) in a cohort of Korean men. This correlation was hypothesized to be associated with decreased alcohol abuse, leading to a healthier lifestyle (*6*). While alcoholism is a significant risk factor for TB (*7*, *8*), we hypothesize that loss of ALDH2 function enhances resistance to bacterial infection independent from lifestyle choices. ALDH2 is responsible for the detoxification of many inflammation-induced aldehydes, including 4-hydroxynonenol (4HNE) and malondialdehyde (MDA) (*9*–*12*). These aldehydes are produced as end products of lipid peroxidation that occurs when macrophages and other innate immune cells generate an oxidative burst to kill pathogens (*11*, *13*–*15*). Additionally, ALDH2, along with alcohol dehydrogenase 5 (ADH5), is vital for the metabolism of endogenous formaldehyde (FA), which is produced via a wide range of cellular processes (*16*, *17*). ALDH2 is situated at a unique metabolic crossroads where it is responsible for the detoxification of numerous reactive aldehydes with wide-ranging physiological effects, further underscoring its importance for maintaining homeostasis during inflammation.

83 Here we demonstrate that loss of ALDH2 function improves control of bacterial infections. We
84 found ALDH2-deficient macrophages produced higher levels of toxic aldehydes and were better
85 able to control *Francisella tularensis* growth. Mice lacking *Aldh2* had enhanced resistance to
86 both *Mycobacterium tuberculosis* and *F. tularensis.* Given that these bacteria were killed by
87 aldehydes normally detoxified by ALDH2, our data suggest that individuals with the *ALDH2*2*
88 allele are protected against bacterial infection through the production of microbicidal aldehydes.
89

90 **ALDH2 rs671 is associated with lower pulmonary tuberculosis risk**

91 To examine the relationship between the *ALDH2*2* mutation (rs671) and TB, we performed a
92 candidate gene analysis. Genotype data of rs671 was available from a collection of 2,030

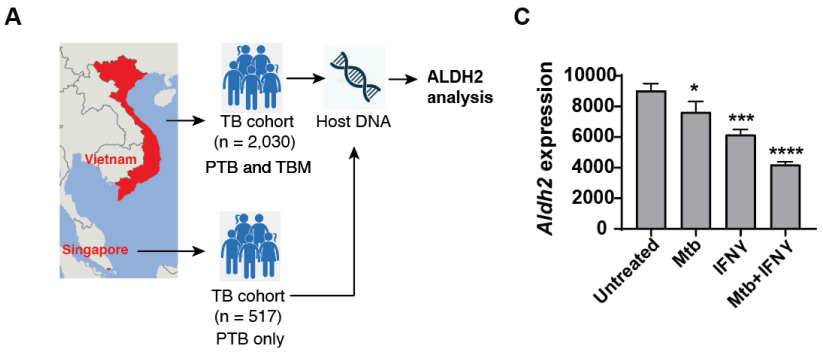

SNP	Dataset (case/control)	Test Allele	Other Allele	OR (95% CI)	P value
rs671	PTB Vietnam (1598/1267)	A	G	0.835 (0.725, 0.962)	0.013
	PTB Singapore (517/24,015)			0.890 (0.775, 1.022)	0.098
	PTB Meta-analysis			**0.863 (0.782, 0.952)**	**0.003**
rs671	TBM Vietnam (407/1138)	A	G	0.972 (0.7841, 1.204)	0.794

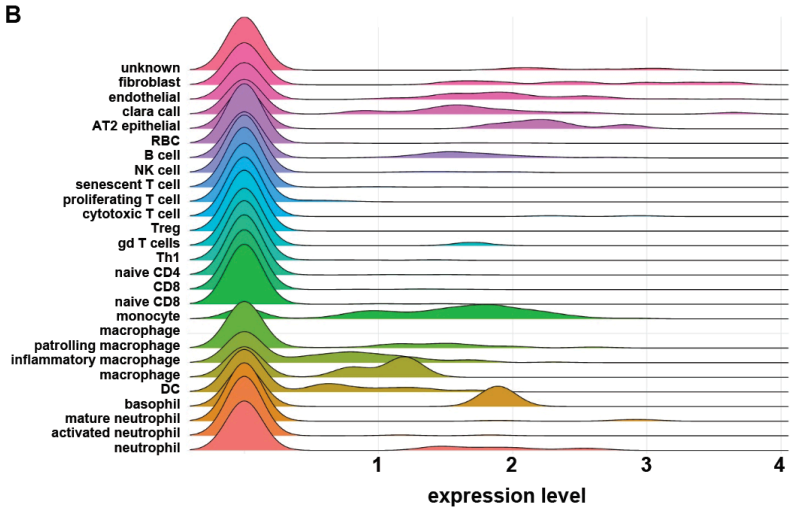

Figure 1. **ALDH2 expression is linked with human disease and immune activation.** A) A candidate gene analysis of the ALDH2 rs671 mutation in pulmonary TB (PTB) patients in Vietnam and Singapore and TB meningitis (TBM) patients in Vietnam. B) *Aldh2* expression in single cell populations of *M. tuberculosis* infected C57BL/6J (B6) mice. C) Normalized bulk RNA expression of B6 bone marrow-derived macrophages (BMDMs) stimulated with IFNγ and/or *M. tuberculosis* H37Rv (n = 3 independent experiments). *, $p < 0.05$, ***, $p < 0.001$, ****, $p < 0.0001$, Unpaired t-test

93 microbiologically confirmed TB patients and 1,263 population control subjects with primary
94 angle closure glaucoma, from Vietnam. Analysis was stratified by clinical phenotype, comparing
95 all TB cases, pulmonary TB (PTB), and TB meningitis (TBM) with ethnically matched population
96 controls (Fig. 1A). We observed a null significant association just above the significance
97 threshold between rs671 and all TB cases [odds ratio/OR (95%CI) = 0.875 (0.764, 1.000), *P* =
98 0.051]. After stratification by clinical phenotype, a significant association was observed between
99 PTB and controls [OR (95%CI) = 0.835 (0.725, 0.962), *P* = 0.013], but not for TBM (Fig. 1A).
100 PTB is the most common clinical manifestation of TB disease and leads to the principal mode of
101 transmission amongst humans. Subsequently, we replicated the association in the Singapore
102 Chinese Health Study (SCHS), which consists of 517 active PTB cases and 24,015 population
103 controls of Singaporean Chinese origin, and then performed a meta-analysis of the PTB
104 datasets from Vietnam and Singapore. The overall association between rs671 and PTB was
105 statistically significant [OR (95% CI) = 0.863 (0.782, 0.952), *P*=0.003, $P_{heterogeneity=0.531}$]. These
106 data, together with the previous published association study (*6*) support the hypothesis that the
107 *ALDH2*2* rs671 mutation is associated with protection against PTB.
108
109 **_Aldh2_ expression in macrophages is downregulated upon inflammatory stimulation**
110 To further examine the link between ALDH2 and *M. tuberculosis*, we examined *Aldh2*
111 expression in the lungs of *M. tuberculosis* infected C57BL/6J ("B6") mice using single cell RNA
112 sequencing (scRNAseq). *Aldh2* expression was observed in macrophage/monocytes
113 populations, dendritic cells, neutrophils, basophils, B cells, pulmonary epithelial and endothelial
114 cells, and fibroblasts (Fig. 1B). Other immune cell types, such as T cells, did not express *Aldh2*
115 (Fig. 1B). Due to the increased levels of *Aldh2* expression in the myeloid compartment, we next
116 sought to determine the effect of IFNγ, which is crucial for macrophage activation and control of
117 *M. tuberculosis* infection (*18*), on *Aldh2* expression. We infected bone marrow-derived
118 macrophages (BMDM) from B6 mice in the presence or absence of IFNγ for 24 hours. As
119 predicted from *in vivo* scRNAseq, *Aldh2* was expressed in unstimulated BMDMs (Fig. 1B-C).
120 Unexpectedly, we found that activation with IFNγ decreased expression of *Aldh2* in both
121 uninfected and *M. tuberculosis*-infected macrophages (Fig. 1C). These results suggest there is
122 a IFNγ induced program to decrease ALDH2 activity and expression during infection.
123
124 **Aldehydes detoxified by ALDH2 kill *M. tuberculosis***
125 Based on the role of ALDH2 in detoxifying inflammation-associated aldehydes, we tested the
126 susceptibility of *M. tuberculosis* to 4HNE, MDA, and FA in axenic culture at physiologically
127 relevant levels. Both 4HNE and MDA can reach micromolar to millimolar intracellular
128 concentrations in inflamed tissues (*10*, *19*, *20*), and FA has been found to reach levels of up to
129 100 μM in the blood (*21–23*). *M. tuberculosis* was sensitive to 4HNE with ten-fold killing
130 observed at 50 μM after six days of exposure and greater than three orders of magnitude of
131 toxicity at 200 μM (Fig. 2A) relative to controls. Similarly, we found that MDA and FA both
132 significantly killed *M. tuberculosis* at 200 μM and 100 μM, respectively (Fig. 2B, 2C). Previous
133 work has reported that bacterial-derived aldehydes sensitize *M. tuberculosis* to nitric oxide (NO)
134 (*24*). NO production by macrophages is required for control of *M. tuberculosis* infection, and is
135 induced by IFNγ (*25*, *26*). We observed that 4HNE and NO together had a synergistic effect
136 against *M. tuberculosis*, with apparent sterilization of the culture occurring at 200 μM 4HNE in

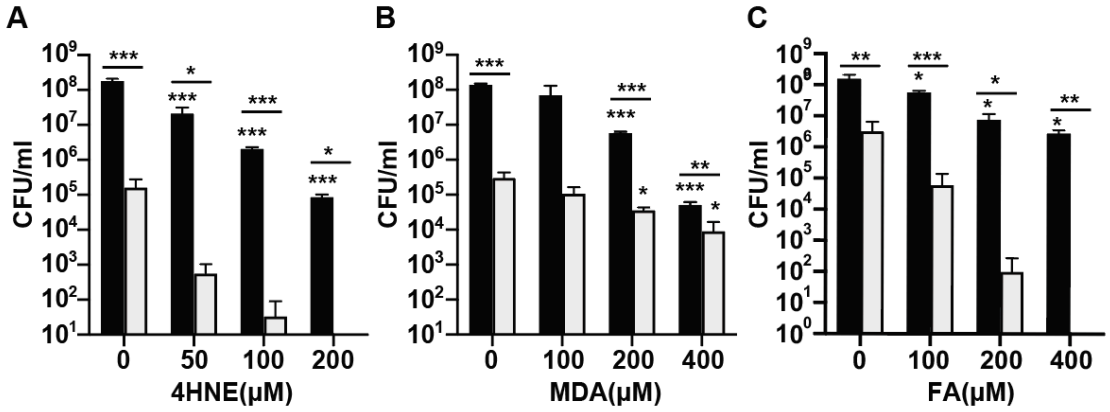

Figure 2. Aldehydes normally detoxified by ALDH2 kill *M. tuberculosis*. *M. tuberculosis* H37Rv killing after six days treatment with physiological levels of A) 4-hydroxynonenal (4HNE), B) malondialdehyde (MDA), or C) formaldehyde (FA), treated in the absence (black bars) or presence of nitric oxide (NO, 3 mM, light grey bars). Comparisons are against the 0 μM-treated condition (n = 2 independent experiments, representative experiment shown). *, $p < 0.05$, **, $p < 0.01$, ***, $p < 0.001$, ****, $p < 0.0001$, Unpaired t-test. Significance is measured comparing the aldehyde treatments against untreated in the no NO condition, the aldehyde treatments against untreated in the plus NO condition, and comparing the same aldehyde concentration +/- NO.

the presence of NO (Fig. 2A). Similarly, we observed that FA and NO synergized to induce killing of *M. tuberculosis*, with sterilization of the culture occurring at 400 μM (Fig. 2C). The presence of NO had less of an impact on treatment with MDA, although some synergy was observed at 200 μM and 400 μM (Fig. 2B).

Macrophages from *Aldh2*-deficient mice produce higher levels of aldehyde but do not exhibit enhanced control of *M. tuberculosis* infection.

We next generated *Aldh2* mutant (*Aldh2*$^{-/-}$) mice using CRISPR-Cas9. Despite being an in-frame deletion, the mutation (12 base pair deletion in exon 12 that encompasses the region where rs671 is found in humans) appeared to be loss of function, as no ALDH2 protein was detectable by immunoblotting (Fig. S1). We tested if immune activation increases aldehyde production by wild-type (WT) macrophages and whether aldehyde production is further enhanced by *Aldh2*-deficiency. Using Mito-RFAP-2, a mitochondrial-targeted ratiometric dye that detects mitochondrial-localized FA with high sensitivity, we found WT macrophages stimulated with IFNγ and PAM3CSK4, a TLR2 agonist, had increased aldehyde levels24 hours after stimulation (Fig. 3A). This stimulation-induced enhancement of aldehyde production in macrophages inversely correlates with *Aldh2* expression, as IFNγ stimulation decreased *Aldh2* levels (Fig. 1C) and increased mitochondrial aldehyde levels (Fig. 3A). *Aldh2*$^{-/-}$ macrophages produced significantly more aldehyde than the WT cells in the absence of immune stimulation (Fig. 3A). However, a significant difference was not observed between stimulated and unstimulated *Aldh2*$^{-/-}$ macrophages, suggesting that aldehyde levels in the *Aldh2*$^{-/-}$ macrophages could not be further increased by external stimulation.

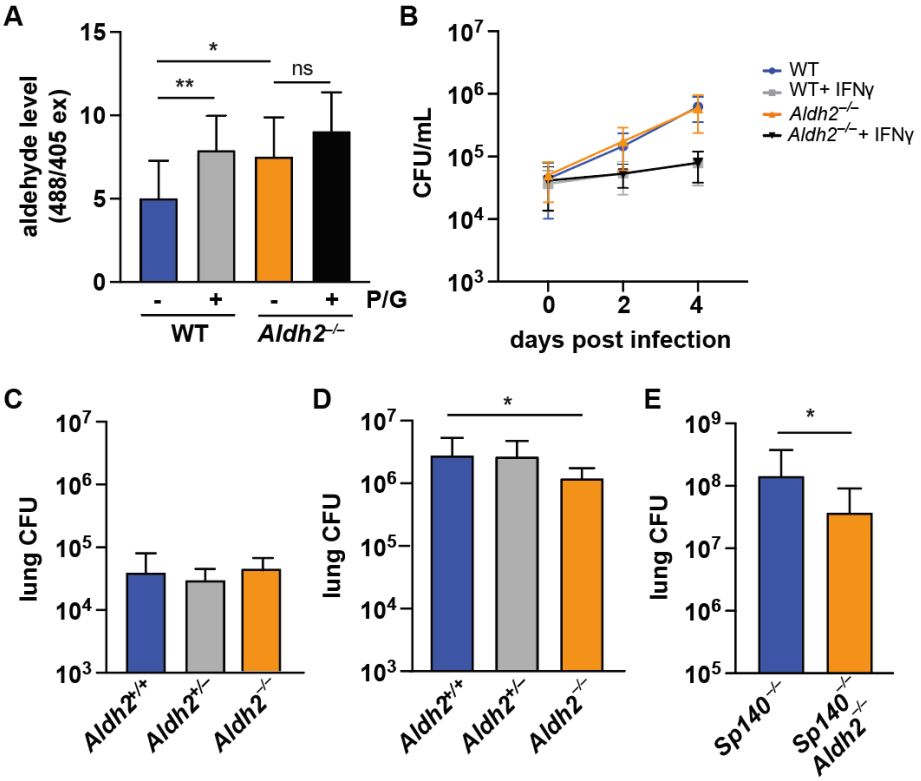

Figure 3. *Aldh2*$^{-/-}$ mice demonstrate improved control of *M. tuberculosis in vivo*. A) B6 and *Aldh2*$^{-/-}$ BMDM mitochondrial-associated formaldehyde levels after 24 hours stimulation with IFNγ and TLR2-agonist PAM3CSK4 *in vitro* (n = 3 independent experiments). B) CFU enumeration of B6 and *Aldh2*$^{-/-}$ BMDMs infected with *M. tuberculosis* LuxErd +/- IFNγ at an MOI: 1 (n = 2 independent experiments). Lung CFU enumeration of aerosol-infected *Aldh2*$^{-/-}$, *Aldh2*$^{+/-}$, and *Aldh2*$^{+/+}$ littermate mice with ≈ 25 CFU *M. tuberculosis* H37Rv C) 14 dpi (n = 2 independent experiments) or D) 28 dpi (n = 3 independent experiments). E) Lung CFU enumeration of aerosol-infected *Sp140*$^{-/-}$ and *Sp140*$^{-/-}$ *Aldh2*$^{-/-}$ mice with ≈ 25 CFU *M. tuberculosis* Erdman 28 dpi (n = 3 independent experiments). *, $p < 0.05$, **, $p < 0.01$, ns = not significant. A and B, Unpaired t-test; C-E, Mann-Whitney test.

Subsequently, we tested whether ALDH2 deficiency enhances control of *M. tuberculosis* by infected macrophages. WT and *Aldh2*$^{-/-}$ macrophages were infected with *M. tuberculosis* at a multiplicity of infection of one bacillus per macrophage (MOI = 1) and bacterial replication was monitored over four days. *M. tuberculosis* replication was identical in WT and *Aldh2*$^{-/-}$ macrophages (Fig. 3B). We observed the expected restriction of *M. tuberculosis* growth after IFNγ activation, but we did not observe significant differences between the WT and *Aldh2*$^{-/-}$ BMDMs (Fig. 3B). Given that *in vitro* conditions do not recapitulate the extent of inflammation, nor the full pathogenesis observed *in vivo*, we performed aerosol infections of *Aldh2*$^{-/-}$ mice to determine the role of ALDH2 in a biologically relevant model of *M. tuberculosis.*

Mice lacking *Aldh2* are protected against *M. tuberculosis* infection

We infected *Aldh2*$^{-/-}$ mice *via* the aerosol route with a low-to-medium dose (~25 colony forming units, CFU) of *M. tuberculosis*, and harvested their lungs for CFU enumeration at various time

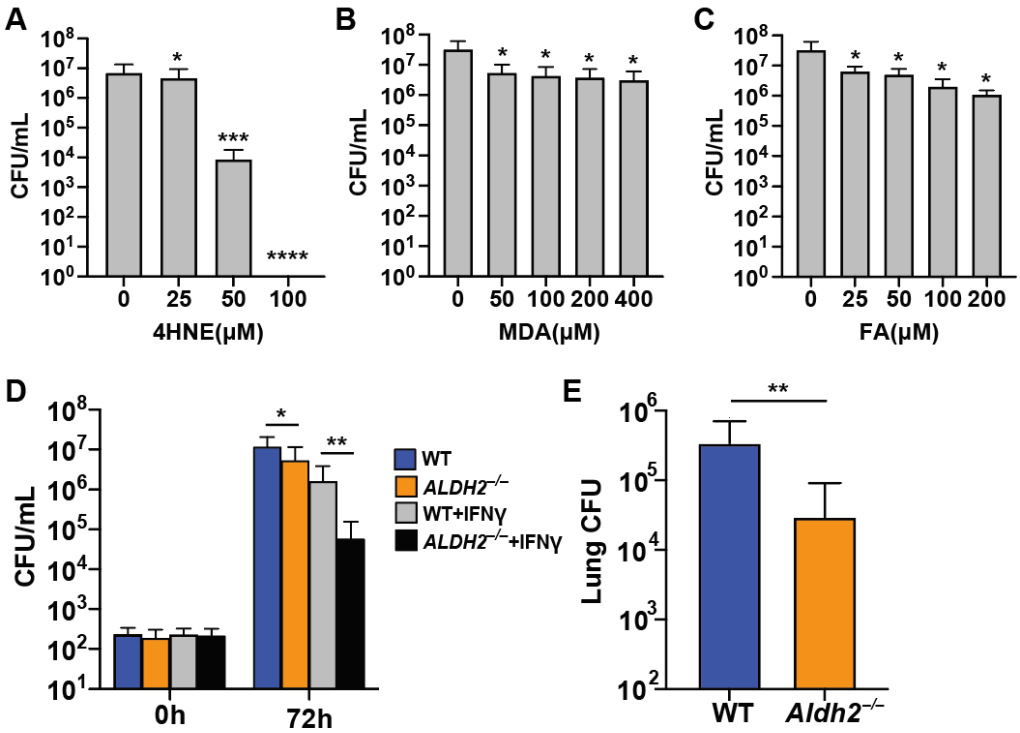

Figure 4. *Aldh2*$^{-/-}$ mice are protected against *F. tularensis* LVS infection. *F. tularensis* LVS killing after 2 hours of treatment with physiological levels of A) 4HNE, B) MDA, or C) FA (n = 2 independent experiments). D) CFU enumeration of B6 and *Aldh2*$^{-/-}$ BMDMs infected with *F. tularensis* LVS +/- IFNγ at an MOI: 0.1 (n = 3 independent experiments, representative experiment shown). E) Lung CFU enumeration of B6 and *Aldh2*$^{-/-}$ mice infected with ≈ 10^6 CFU *F. tularensis* LVS 5 dpi (n = 2 independent experiments). *, $p < 0.05$, **, $p < 0.01$, ****, $p < 0.0001$, ns = not significant. A-D, Unpaired t-test; E, Mann-Whitney test.

points. At 14 days post infection (dpi), we observed no difference in the ability of *Aldh2*$^{-/-}$ mice to control pulmonary infection when compared with littermate controls (Fig. 3C). However, at 28 dpi, we observed a significant difference between *Aldh2*$^{-/-}$ mice and the WT mice, wherein *Aldh2*$^{-/-}$ mice had significantly lower bacterial burdens (Fig. 3D). The adaptive immune response is typically observed after 14 dpi in mice, where increased IFNγ signaling results from T cell migration to the site of infection; this result suggests that sustained T cell-mediated IFNγ signaling could contribute to the improved control observed by the *Aldh2*$^{-/-}$ mice at 28 dpi by increasing local aldehyde production.

B6 mice are relatively resistant to infection with *M. tuberculosis* (*27*, *28*). We hypothesized that the protective effect of ALDH2 could be more dramatic in the context of a susceptible strain in which a loss of bacterial control correlates with destructive inflammatory responses in the lung, as well as in a setting of increased aldehyde load (Fig. S2). To test this hypothesis, we generated *Aldh2*$^{-/-}$ mice on the background of *Sp140* deficiency. *Sp140*$^{-/-}$ mice have type I IFN-driven susceptibility to disease and severe bacterial burden during *M. tuberculosis* infection (*29*). We infected *Aldh2*$^{-/-}$ *Sp140*$^{-/-}$ and parental *Sp140*$^{-/-}$ mice with *M. tuberculosis*. Both

genotypes had increased overall lung CFU relative to *Aldh2*$^{-/-}$ and WT mice due to the known susceptibility of the *Sp140*$^{-/-}$ background (Fig. 3E). Similar to the wild-type B6 model, we observed significantly fewer CFU in the *Aldh2*$^{-/-}$*Sp140*$^{-/-}$ mice when compared to parental *Sp140*$^{-/-}$ animals at 28 dpi (Fig. 3E). Thus, even in the presence of a host-detrimental inflammatory type I IFN response, disruption of *Aldh2* had a protective effect against *M. tuberculosis* infection.

Aldh2$^{-/-}$ mice are protected against *Francisella* infection

It is established that other bacterial species are susceptible to metabolic aldehydes, and that bacteria have various aldehyde-detoxification pathways to protect against aldehyde exposure (*30*, *31*). Previous work demonstrated variable susceptibility of numerous pathogens to 4HNE *in vitro* (*30*). While *Listeria monocytogenes* is relatively resistant to 4HNE, *Francisella novicida* is highly susceptible. Similarly, we observed that the live vaccine strain (LVS) of *Francisella tularensis* was more susceptible to aldehydes, including 4HNE, MDA, and FA, than *M. tuberculosis* (Fig. 4A-C). *F. tularensis* LVS was sensitive to 4HNE with almost three orders of magnitude of bacterial killing at 50 μM, and significant killing was also observed at 25 μM FA and 50 μM MDA (Fig. 4A-C). Due to the sensitivity of *F. tularensis* LVS to aldehydes known to be detoxified by ALDH2, we tested LVS growth in WT and *Aldh2*$^{-/-}$ macrophages. We observed restriction of LVS growth in IFNγ-activated BMDMs, and significantly fewer CFU in the IFNγ-activated *Aldh2*$^{-/-}$ macrophages when compared to the WT macrophages (Fig. 4D), supporting a cell-intrinsic role for aldehydes on pathogen control. Consistent with this observation and our data with *M. tuberculosis*, we found significantly fewer CFU in the lungs of *Aldh2*$^{-/-}$ mice when compared to WT mice infected with *F. tularensis* LVS (Fig. 4E). Overall, these results support our hypothesis that increased levels of inflammation-induced aldehydes are protective during infection by intracellular pathogens.

Discussion

Lipid peroxidation end products metabolized by ALDH2, such as 4HNE and MDA, have been implicated in serious health disorders, and are typically produced as a result of reactive oxidative bursts interacting with intracellular lipid membranes and other inflammatory processes. Despite the role of ALDH2 as a detoxification enzyme for inflammation-induced byproducts, we found that during inflammation, ALDH2 expression is counterintuitively decreased, leading to increased accumulation of aldehyde. We have demonstrated that 4HNE, MDA, and FA, are directly toxic to *M. tuberculosis* and *F. tularensis* LVS *in vitro* and work synergistically with other antimicrobial factors (e.g., NO) against *M. tuberculosis*. However, accumulation of 4HNE and MDA above homeostatic levels can also induce mitochondrial cell death pathways, such as apoptosis, which has been shown to be advantageous for clearance of *M. tuberculosis* infection (*32*–*34*); therefore, it is possible that the accumulation of these aldehydes may indirectly lead to *M. tuberculosis*-killing through intrinsic apoptosis. Future studies will focus on the elucidation of the mechanism of aldehyde-mediated killing, as well as the identification and characterization of the pathway responsible for the generation of these aldehydes during inflammation.

In vivo, the lack of host ALDH2 provides host-mediated protection against infection, indicating that these aldehydes are likely part of the host armory of antimicrobial factors working in tandem to fight infection by intracellular pathogens. The *ALDH2*2* allele is predicted to have evolved

about 3,000 years ago (*35*) and is predominantly found in individuals of east Asian descent; interestingly, the evolution of lineage 2 (also known as the W/Beijing lineage) of *M. tuberculosis* arose between 2,000 – 7,000 years ago (*35*, *36*), and this lineage is more frequent in East Asia. Together with previous data (*6*), we have found a positive association between individuals harboring the rs671 A allele (*ALDH2*2* allele) and PTB, suggesting that there may have been evolutionary pressure selecting for this allele in environments where TB transmission is prevalent. Lineage 2 strains are known to have increased transmissibility, be hypervirulent, and possess increased drug resistance, in addition to having a higher mutation rate (*37–40*); this propensity may also facilitate its survival against antimicrobial stresses, such as toxic aldehydes. Further research is needed to examine the evolutionary interplay between *ALDH2*2* and lineage 2 strains and to probe for select mutations that confer resistance to aldehyde stress or other cell death-associated antimicrobial stresses. However, this resistance to infection is not limited to *M. tuberculosis*, as we observed an even greater protective effect in *Aldh2*$^{-/-}$ mice against infection by *F. tularensis* LVS. Therefore, we propose that the *ALDH2*2* allele may have evolved to be broadly protective against a wide range of bacterial infections, including those brought on by highly evolved human pathogens (e.g., *M. tuberculosis*)(*41*, *42*) and less evolved pathogens (e.g., *F. tularensis*). The protective association between *ALDH2*2* and PTB may in fact be the result of a positive selective pressure to maintain the *ALDH2*2* allele in response to bacterial infection generally. While ALDH2 plays an important role in the detoxification of metabolic aldehydes, we demonstrate that its absence provides a host-protective role against infection. This could be an example of balancing selection, of which sickle cell anemia and malaria in Africa is a classic example (*43–45*). We speculate that the advantage afforded by *ALDH2*2* to enhance response to bacterial infection could contribute to the maintenance of this mutation in the East Asian population despite its detrimental effects on human health (*4*, *5*).

References:

1. C.-H. Chen, B. R. Kraemer, D. Mochly-Rosen, ALDH2 variance in disease and populations. *Dis. Model. Mech.* **15** (2022), doi:10.1242/dmm.049601.

2. C. Impraim, G. Wang, A. Yoshida, Structural mutation in a major human aldehyde dehydrogenase gene results in loss of enzyme activity. *Am. J. Hum. Genet.* **34**, 837–841 (1982).

3. S. Harada, D. P. Agarwal, H. W. Goedde, Aldehyde dehydrogenase deficiency as cause of facial flushing reaction to alcohol in Japanese. *Lancet*. **2**, 982 (1981).

4. E. R. Gross, V. O. Zambelli, B. A. Small, J. C. B. Ferreira, C.-H. Chen, D. Mochly-Rosen, A personalized medicine approach for Asian Americans with the aldehyde dehydrogenase 2*2 variant. *Annu. Rev. Pharmacol. Toxicol.* **55**, 107–127 (2015).

5. C.-H. Chen, J. C. B. Ferreira, E. R. Gross, D. Mochly-Rosen, Targeting aldehyde dehydrogenase 2: new therapeutic opportunities. *Physiol. Rev.* **94**, 1–34 (2014).

273 6. S. K. Park, C.-S. Park, H.-S. Lee, K. S. Park, B. L. Park, H. S. Cheong, H. D. Shin,
274 Functional polymorphism in aldehyde dehydrogenase-2 gene associated with risk of
275 tuberculosis. *BMC Med. Genet.* **15**, 40 (2014).

276 7. J. Rehm, A. V. Samokhvalov, M. G. Neuman, R. Room, C. Parry, K. Lönnroth, J. Patra, V.
277 Poznyak, S. Popova, The association between alcohol use, alcohol use disorders and
278 tuberculosis (TB). A systematic review. *BMC Public Health*. **9**, 450 (2009).

279 8. S. Imtiaz, K. D. Shield, M. Roerecke, A. V. Samokhvalov, K. Lönnroth, J. Rehm, Alcohol
280 consumption as a risk factor for tuberculosis: meta-analyses and burden of disease. *Eur.*
281 *Respir. J.* **50** (2017), doi:10.1183/13993003.00216-2017.

282 9. G. Barrera, S. Pizzimenti, E. S. Ciamporcero, M. Daga, C. Ullio, A. Arcaro, G. P.
283 Cetrangolo, C. Ferretti, C. Dianzani, A. Lepore, F. Gentile, Role of 4-hydroxynonenal-
284 protein adducts in human diseases. *Antioxid. Redox Signal.* **22**, 1681–1702 (2015).

285 10. M. Shoeb, N. H. Ansari, S. K. Srivastava, K. V. Ramana, 4-Hydroxynonenal in the
286 pathogenesis and progression of human diseases. *Curr. Med. Chem.* **21**, 230–237 (2014).

287 11. R. J. Schaur, W. Siems, N. Bresgen, P. M. Eckl, 4-Hydroxy-nonenal-A Bioactive Lipid
288 Peroxidation Product. *Biomolecules*. **5**, 2247–2337 (2015).

289 12. E. J. Anderson, L. A. Katunga, M. S. Willis, Mitochondria as a source and target of lipid
290 peroxidation products in healthy and diseased heart. *Clin. Exp. Pharmacol. Physiol.* **39**,
291 179–193 (2012).

292 13. M. Breitzig, C. Bhimineni, R. Lockey, N. Kolliputi, 4-Hydroxy-2-nonenal: a critical target in
293 oxidative stress? *Am. J. Physiol. Cell Physiol.* **311**, C537–C543 (2016).

294 14. B. Yoval-Sánchez, J. S. Rodríguez-Zavala, Differences in susceptibility to inactivation of
295 human aldehyde dehydrogenases by lipid peroxidation byproducts. *Chem. Res. Toxicol.*
296 **25**, 722–729 (2012).

297 15. A. Ayala, M. F. Muñoz, S. Argüelles, Lipid peroxidation: production, metabolism, and
298 signaling mechanisms of malondialdehyde and 4-hydroxy-2-nonenal. *Oxid. Med. Cell.*
299 *Longev.* **2014**, 360438 (2014).

300 16. F. A. Dingler, M. Wang, A. Mu, C. L. Millington, N. Oberbeck, S. Watcham, L. B. Pontel, A.
301 N. Kamimae-Lanning, F. Langevin, C. Nadler, R. L. Cordell, P. S. Monks, R. Yu, N. K.
302 Wilson, A. Hira, K. Yoshida, M. Mori, Y. Okamoto, Y. Okuno, H. Muramatsu, Y. Shiraishi,
303 M. Kobayashi, T. Moriguchi, T. Osumi, M. Kato, S. Miyano, E. Ito, S. Kojima, H. Yabe, M.
304 Yabe, K. Matsuo, S. Ogawa, B. Göttgens, M. R. G. Hodskinson, M. Takata, K. J. Patel, Two
305 Aldehyde Clearance Systems Are Essential to Prevent Lethal Formaldehyde Accumulation
306 in Mice and Humans. *Mol. Cell*. **80**, 996-1012.e9 (2020).

307 17. J. Nakamura, D. W. Holley, T. Kawamoto, S. J. Bultman, The failure of two major
308 formaldehyde catabolism enzymes (ADH5 and ALDH2) leads to partial synthetic lethality in
309 C57BL/6 mice. *Genes Environ*. **42**, 21 (2020).

310 18. J. L. Flynn, J. Chan, K. J. Triebold, D. K. Dalton, T. A. Stewart, B. R. Bloom, An essential
311 role for interferon gamma in resistance to Mycobacterium tuberculosis infection. *J. Exp.*
312 *Med.* **178**, 2249–2254 (1993).

313 19. H. Esterbauer, R. J. Schaur, H. Zollner, Chemistry and biochemistry of 4-hydroxynonenal,
314 malonaldehyde and related aldehydes. *Free Radic. Biol. Med.* **11**, 81–128 (1991).

315 20. X. Wang, X. G. Lei, J. Wang, Malondialdehyde regulates glucose-stimulated insulin
316 secretion in murine islets via TCF7L2-dependent Wnt signaling pathway. *Mol. Cell.*
317 *Endocrinol.* **382**, 8–16 (2014).

318 21. G. Burgos-Barragan, N. Wit, J. Meiser, F. A. Dingler, M. Pietzke, L. Mulderrig, L. B. Pontel,
319 I. V. Rosado, T. F. Brewer, R. L. Cordell, P. S. Monks, C. J. Chang, A. Vazquez, K. J. Patel,
320 Mammals divert endogenous genotoxic formaldehyde into one-carbon metabolism. *Nature*.
321 **548**, 549–554 (2017).

322 22. H. D. Heck, M. Casanova-Schmitz, P. B. Dodd, E. N. Schachter, T. J. Witek, T. Tosun,
323 Formaldehyde (CH2O) concentrations in the blood of humans and Fischer-344 rats
324 exposed to CH2O under controlled conditions. *Am. Ind. Hyg. Assoc. J.* **46**, 1–3 (1985).

325 23. W. Luo, H. Li, Y. Zhang, C. Y. Ang, Determination of formaldehyde in blood plasma by
326 high-performance liquid chromatography with fluorescence detection. *J. Chromatogr. B*
327 *Biomed. Sci. Appl.* **753**, 253–257 (2001).

328 24. M. I. Samanovic, S. Tu, O. Novák, L. M. Iyer, F. E. McAllister, L. Aravind, S. P. Gygi, S. R.
329 Hubbard, M. Strnad, K. H. Darwin, Proteasomal control of cytokinin synthesis protects
330 Mycobacterium tuberculosis against nitric oxide. *Mol. Cell*. **57**, 984–994 (2015).

331 25. J. Chan, Y. Xing, R. S. Magliozzo, B. R. Bloom, Killing of virulent Mycobacterium
332 tuberculosis by reactive nitrogen intermediates produced by activated murine
333 macrophages. *J. Exp. Med.* **175**, 1111–1122 (1992).

334 26. J. D. MacMicking, R. J. North, R. LaCourse, J. S. Mudgett, S. K. Shah, C. F. Nathan,
335 Identification of nitric oxide synthase as a protective locus against tuberculosis. *Proc. Natl.*
336 *Acad. Sci. U. S. A.* **94**, 5243–5248 (1997).

337 27. A. M. Cooper, Mouse model of tuberculosis. *Cold Spring Harb. Perspect. Med.* **5**, a018556
338 (2014).

339 28. E. Medina, R. J. North, Resistance ranking of some common inbred mouse strains to
340 Mycobacterium tuberculosis and relationship to major histocompatibility complex haplotype
341 and Nramp1 genotype. *Immunology*. **93**, 270–274 (1998).

342 29. D. X. Ji, K. C. Witt, D. I. Kotov, S. R. Margolis, A. Louie, V. Chevée, K. J. Chen, M. M.
343 Gaidt, H. S. Dhaliwal, A. Y. Lee, S. L. Nishimura, D. S. Zamboni, I. Kramnik, D. A. Portnoy,
344 K. H. Darwin, R. E. Vance, Role of the transcriptional regulator SP140 in resistance to
345 bacterial infections via repression of type I interferons. *Elife*. **10** (2021),
346 doi:10.7554/eLife.67290.

347 30. H. Tabakh, A. P. McFarland, M. K. Thomason, A. J. Pollock, R. C. Glover, S. A. Zaver, J. J.
348 Woodward, 4-Hydroxy-2-nonenal antimicrobial toxicity is neutralized by an intracellular
349 pathogen. *Elife*. **10** (2021), doi:10.7554/eLife.59295.

350 31. A. Anaya-Sanchez, Y. Feng, J. C. Berude, D. A. Portnoy, Detoxification of methylglyoxal by
351 the glyoxalase system is required for glutathione availability and virulence activation in
352 Listeria monocytogenes. *PLoS Pathog.* **17**, e1009819 (2021).

32. S. Dalleau, M. Baradat, F. Guéraud, L. Huc, Cell death and diseases related to oxidative stress: 4-hydroxynonenal (HNE) in the balance. *Cell Death Differ.* **20**, 1615–1630 (2013).

33. S. M. Behar, C. J. Martin, M. G. Booty, T. Nishimura, X. Zhao, H.-X. Gan, M. Divangahi, H. G. Remold, Apoptosis is an innate defense function of macrophages against Mycobacterium tuberculosis. *Mucosal Immunol.* **4**, 279–287 (2011).

34. M. Chen, H. Gan, H. G. Remold, A mechanism of virulence: virulent Mycobacterium tuberculosis strain H37Rv, but not attenuated H37Ra, causes significant mitochondrial inner membrane disruption in macrophages leading to necrosis. *J. Immunol.* **176**, 3707–3716 (2006).

35. Q. Liu, A. Ma, L. Wei, Y. Pang, B. Wu, T. Luo, Y. Zhou, H.-X. Zheng, Q. Jiang, M. Gan, T. Zuo, M. Liu, C. Yang, L. Jin, I. Comas, S. Gagneux, Y. Zhao, C. S. Pepperell, Q. Gao, China's tuberculosis epidemic stems from historical expansion of four strains of Mycobacterium tuberculosis. *Nat Ecol Evol*. **2**, 1982–1992 (2018).

36. M. Merker, C. Blin, S. Mona, N. Duforet-Frebourg, S. Lecher, E. Willery, M. G. B. Blum, S. Rüsch-Gerdes, I. Mokrousov, E. Aleksic, C. Allix-Béguec, A. Antierens, E. Augustynowicz-Kopeć, M. Ballif, F. Barletta, H. P. Beck, C. E. Barry 3rd, M. Bonnet, E. Borroni, I. Campos-Herrero, D. Cirillo, H. Cox, S. Crowe, V. Crudu, R. Diel, F. Drobniewski, M. Fauville-Dufaux, S. Gagneux, S. Ghebremichael, M. Hanekom, S. Hoffner, W.-W. Jiao, S. Kalon, T. A. Kohl, I. Kontsevaya, T. Lillebæk, S. Maeda, V. Nikolayevskyy, M. Rasmussen, N. Rastogi, S. Samper, E. Sanchez-Padilla, B. Savic, I. C. Shamputa, A. Shen, L.-H. Sng, P. Stakenas, K. Toit, F. Varaine, D. Vukovic, C. Wahl, R. Warren, P. Supply, S. Niemann, T. Wirth, Evolutionary history and global spread of the Mycobacterium tuberculosis Beijing lineage. *Nat. Genet.* **47**, 242–249 (2015).

37. M. Hanekom, N. C. Gey van Pittius, C. McEvoy, T. C. Victor, P. D. Van Helden, R. M. Warren, Mycobacterium tuberculosis Beijing genotype: a template for success. *Tuberculosis* . **91**, 510–523 (2011).

38. I. Parwati, R. van Crevel, D. van Soolingen, Possible underlying mechanisms for successful emergence of the Mycobacterium tuberculosis Beijing genotype strains. *Lancet Infect. Dis.* **10**, 103–111 (2010).

39. K. E. Holt, P. McAdam, P. V. K. Thai, N. T. T. Thuong, D. T. M. Ha, N. N. Lan, N. H. Lan, N. T. Q. Nhu, H. T. Hai, V. T. N. Ha, G. Thwaites, D. J. Edwards, A. P. Nath, K. Pham, D. B. Ascher, J. Farrar, C. C. Khor, Y. Y. Teo, M. Inouye, M. Caws, S. J. Dunstan, Frequent transmission of the Mycobacterium tuberculosis Beijing lineage and positive selection for the EsxW Beijing variant in Vietnam. *Nat. Genet.* **50**, 849–856 (2018).

40. C. B. Ford, R. R. Shah, M. K. Maeda, S. Gagneux, M. B. Murray, T. Cohen, J. C. Johnston, J. Gardy, M. Lipsitch, S. M. Fortune, Mycobacterium tuberculosis mutation rate estimates from different lineages predict substantial differences in the emergence of drug-resistant tuberculosis. *Nat. Genet.* **45**, 784–790 (2013).

41. S. Gagneux, Host-pathogen coevolution in human tuberculosis. *Philos. Trans. R. Soc. Lond. B Biol. Sci.* **367**, 850–859 (2012).

42. D. Brites, S. Gagneux, Co-evolution of Mycobacterium tuberculosis and Homo sapiens. *Immunol. Rev.* **264**, 6–24 (2015).

43. A. Ferreira, I. Marguti, I. Bechmann, V. Jeney, A. Chora, N. R. Palha, S. Rebelo, A. Henri, Y. Beuzard, M. P. Soares, Sickle hemoglobin confers tolerance to Plasmodium infection. *Cell*. **145**, 398–409 (2011).

44. K. Croke, D. S. Ishengoma, F. Francis, J. Makani, M. L. Kamugisha, J. Lusingu, M. Lemnge, H. Larreguy, G. Fink, B. P. Mmbando, Relationships between sickle cell trait, malaria, and educational outcomes in Tanzania. *BMC Infect. Dis.* **17**, 568 (2017).

45. G. Pasvol, D. J. Weatherall, R. J. Wilson, Cellular mechanism for the protective effect of haemoglobin S against P. falciparum malaria. *Nature*. **274**, 701–703 (1978).

46. R. M. Quadros, H. Miura, D. W. Harms, H. Akatsuka, T. Sato, T. Aida, R. Redder, G. P. Richardson, Y. Inagaki, D. Sakai, S. M. Buckley, P. Seshacharyulu, S. K. Batra, M. A. Behlke, S. A. Zeiner, A. M. Jacobi, Y. Izu, W. B. Thoreson, L. D. Urness, S. L. Mansour, M. Ohtsuka, C. B. Gurumurthy, Easi-CRISPR: a robust method for one-step generation of mice carrying conditional and insertion alleles using long ssDNA donors and CRISPR ribonucleoproteins. *Genome Biol.* **18**, 92 (2017).

47. T. F. Brewer, G. Burgos-Barragan, N. Wit, K. J. Patel, C. J. Chang, A 2-aza-Cope reactivity-based platform for ratiometric fluorescence imaging of formaldehyde in living cells. *Chem. Sci.* **8**, 4073–4081 (2017).

48. J. Ohata, K. J. Bruemmer, C. J. Chang, Activity-Based Sensing Methods for Monitoring the Reactive Carbon Species Carbon Monoxide and Formaldehyde in Living Systems. *Acc. Chem. Res.* **52**, 2841–2848 (2019).

49. M. M. Ravesloot-Chavez, E. Van Dis, D. Fox, X. H. Nguyenla, S. L. Rawal, M. A. Ballinger, H. Thomas, D. I. Kotov, R. Vance, M. Nachman, S. Stanley, Tuberculosis susceptibility in genetically diverse mice reveals functional diversity of neutrophils. *bioRxiv* (2023), p. 2023.06.29.547125, , doi:10.1101/2023.06.29.547125.

50. K. R. Petersen, D. A. Streett, A. T. Gerritsen, S. S. Hunter, M. L. Settles, "Super deduper, fast PCR duplicate detection in fastq files" in *Proceedings of the 6th ACM Conference on Bioinformatics, Computational Biology and Health Informatics* (Association for Computing Machinery, New York, NY, USA, 2015), *BCB '15*, pp. 491–492.

51. A. Frankish, M. Diekhans, A.-M. Ferreira, R. Johnson, I. Jungreis, J. Loveland, J. M. Mudge, C. Sisu, J. Wright, J. Armstrong, I. Barnes, A. Berry, A. Bignell, S. Carbonell Sala, J. Chrast, F. Cunningham, T. Di Domenico, S. Donaldson, I. T. Fiddes, C. García Girón, J. M. Gonzalez, T. Grego, M. Hardy, T. Hourlier, T. Hunt, O. G. Izuogu, J. Lagarde, F. J. Martin, L. Martínez, S. Mohanan, P. Muir, F. C. P. Navarro, A. Parker, B. Pei, F. Pozo, M. Ruffier, B. M. Schmitt, E. Stapleton, M.-M. Suner, I. Sycheva, B. Uszczynska-Ratajczak, J. Xu, A. Yates, D. Zerbino, Y. Zhang, B. Aken, J. S. Choudhary, M. Gerstein, R. Guigó, T. J. P. Hubbard, M. Kellis, B. Paten, A. Reymond, M. L. Tress, P. Flicek, GENCODE reference annotation for the human and mouse genomes. *Nucleic Acids Res.* **47**, D766–D773 (2019).

52. A. Dobin, C. A. Davis, F. Schlesinger, J. Drenkow, C. Zaleski, S. Jha, P. Batut, M. Chaisson, T. R. Gingeras, STAR: ultrafast universal RNA-seq aligner. *Bioinformatics*. **29**, 15–21 (2013).

53. J. A. Shah, A. J. Warr, A. D. Graustein, A. Saha, S. J. Dunstan, N. T. T. Thuong, G. E. Thwaites, M. Caws, P. V. K. Thai, N. D. Bang, T. T. H. Chau, C. C. Khor, Z. Li, M. Hibberd,

X. Chang, F. K. Nguyen, C. A. Hernandez, M. A. Jones, C. M. Sassetti, K. A. Fitzgerald, M. Musvosvi, A. Gela, W. A. Hanekom, M. Hatherill, T. J. Scriba, T. R. Hawn, REL and BHLHE40 Variants Are Associated with IL-12 and IL-10 Responses and Tuberculosis Risk. *J. Immunol.* **208**, 1352–1361 (2022).

54. A. D. Heemskerk, N. D. Bang, N. T. H. Mai, T. T. H. Chau, N. H. Phu, P. P. Loc, N. V. V. Chau, T. T. Hien, N. H. Dung, N. T. N. Lan, N. H. Lan, N. N. Lan, L. T. Phong, N. N. Vien, N. Q. Hien, N. T. B. Yen, D. T. M. Ha, J. N. Day, M. Caws, L. Merson, T. T. V. Thinh, M. Wolbers, G. E. Thwaites, J. J. Farrar, Intensified Antituberculosis Therapy in Adults with Tuberculous Meningitis. *N. Engl. J. Med.* **374**, 124–134 (2016).

55. P. V. K. Thai, D. T. M. Ha, N. T. Hanh, J. Day, S. Dunstan, N. T. Q. Nhu, V. S. Kiet, N. H. Lan, N. H. Dung, N. T. N. Lan, N. T. Thuong, N. N. Lan, P. T. T. Liễu, N. T. Hồng, Đ. C. Điệp, N. T. K. Thanh, N. V. Hội, N. V. Nghĩa, T. N. Đại, H. Q. Minh, N. V. Thơm, J. Farrar, M. Caws, Bacterial risk factors for treatment failure and relapse among patients with isoniazid resistant tuberculosis. *BMC Infect. Dis.* **18**, 112 (2018).

56. G. E. Thwaites, D. B. Nguyen, H. D. Nguyen, T. Q. Hoang, T. T. O. Do, T. C. T. Nguyen, Q. H. Nguyen, T. T. Nguyen, N. H. Nguyen, T. N. L. Nguyen, N. L. Nguyen, H. D. Nguyen, N. T. Vu, H. H. Cao, T. H. C. Tran, P. M. Pham, T. D. Nguyen, K. Stepniewska, N. J. White, T. H. Tran, J. J. Farrar, Dexamethasone for the treatment of tuberculous meningitis in adolescents and adults. *N. Engl. J. Med.* **351**, 1741–1751 (2004).

57. C. C. Khor, T. Do, H. Jia, M. Nakano, R. George, K. Abu-Amero, R. Duvesh, L. J. Chen, Z. Li, M. E. Nongpiur, S. A. Perera, C. Qiao, H.-T. Wong, H. Sakai, M. Barbosa de Melo, M.-C. Lee, A. S. Chan, Y. Azhany, T. L. H. Dao, Y. Ikeda, R. A. Perez-Grossmann, T. Zarnowski, A. C. Day, J. B. Jonas, P. O. S. Tam, T. A. Tran, H. Ayub, F. Akhtar, S. Micheal, P. T. K. Chew, L. A. Aljasim, T. Dada, T. T. Luu, M. S. Awadalla, N. Kitnarong, B. Wanichwecharungruang, Y. Y. Aung, J. Mohamed-Noor, S. Vijayan, S. Sarangapani, R. Husain, A. Jap, M. Baskaran, D. Goh, D. H. Su, H. Wang, V. K. Yong, L. W. Yip, T. B. Trinh, M. Makornwattana, T. T. Nguyen, E. U. Leuenberger, K.-H. Park, W. A. Wiyogo, R. S. Kumar, C. Tello, Y. Kurimoto, S. S. Thapa, K. Pathanapitoon, J. F. Salmon, Y. H. Sohn, A. Fea, M. Ozaki, J. S. M. Lai, V. Tantisevi, C. C. Khaing, T. Mizoguchi, S. Nakano, C.-Y. Kim, G. Tang, S. Fan, R. Wu, H. Meng, T. T. G. Nguyen, T. D. Tran, M. Ueno, J. M. Martinez, N. Ramli, Y. M. Aung, R. D. Reyes, S. A. Vernon, S. K. Fang, Z. Xie, X. Y. Chen, J. N. Foo, K. S. Sim, T. T. Wong, D. T. Quek, R. Venkatesh, S. Kavitha, S. R. Krishnadas, N. Soumittra, B. Shantha, B.-A. Lim, J. Ogle, J. P. C. de Vasconcellos, V. P. Costa, R. Y. Abe, B. B. de Souza, C. C. Sng, M. C. Aquino, E. Kosior-Jarecka, G. B. Fong, V. C. Tamanaja, R. Fujita, Y. Jiang, N. Waseem, S. Low, H. N. Pham, S. Al-Shahwan, E. R. Craven, M. I. Khan, R. Dada, K. Mohanty, M. A. Faiq, A. W. Hewitt, K. P. Burdon, E. H. Gan, A. Prutthipongsit, T. Patthanathamrongkasem, M. A. T. Catacutan, I. R. Felarca, C. S. Liao, E. Rusmayani, V. W. Istiantoro, G. Consolandi, G. Pignata, C. Lavia, P. Rojanapongpun, L. Mangkornkanokpong, S. Chansangpetch, J. C. H. Chan, B. N. K. Choy, J. W. H. Shum, H. M. Than, K. T. Oo, A. T. Han, V. H. Yong, X.-Y. Ng, S. R. Goh, Y. F. Chong, M. L. Hibberd, M. Seielstad, E. Png, S. J. Dunstan, N. V. V. Chau, J. Bei, Y. X. Zeng, A. Karkey, B. Basnyat, F. Pasutto, D. Paoli, P. Frezzotti, J. J. Wang, P. Mitchell, J. H. Fingert, R. R. Allingham, M. A. Hauser, S. T. Lim, S. H. Chew, R. P. Ebstein, A. Sakuntabhai, K. H. Park, J. Ahn, G. Boland, H. Snippe, R. Stead, R. Quino, S. N. Zaw, U. Lukasik, R. Shetty, M. Zahari, H. W. Bae, N. L. Oo, T. Kubota, A. Manassakorn, W. L. Ho, L. Dallorto, Y. H. Hwang, C. A. Kiire, M. Kuroda, Z. E. Djamal, J. I. M. Peregrino, A. Ghosh, J. W. Jeoung, T. S. Hoan, N. Srisamran, T. Sandragasu, S. H. Set, V. H. Doan, S. S.

484 Bhattacharya, C.-L. Ho, D. T. Tan, R. Sihota, S.-C. Loon, K. Mori, S. Kinoshita, A. I. den
485 Hollander, R. Qamar, Y.-X. Wang, Y. Y. Teo, E.-S. Tai, C. Hartleben-Matkin, D. Lozano-
486 Giral, S. M. Saw, C.-Y. Cheng, J. C. Zenteno, C. P. Pang, H. T. T. Bui, O. Hee, J. E. Craig,
487 D. P. Edward, M. Yonahara, J. M. Neto, M. L. Guevara-Fujita, L. Xu, R. Ritch, A. T. Liza-
488 Sharmini, T. Y. Wong, S. Al-Obeidan, N. H. Do, P. Sundaresan, C. C. Tham, P. J. Foster,
489 L. Vijaya, K. Tashiro, E. N. Vithana, N. Wang, T. Aung, Genome-wide association study
490 identifies five new susceptibility loci for primary angle closure glaucoma. *Nat. Genet.* **48**,
491 556–562 (2016).

492 58. S. J. Dunstan, N. T. Hue, B. Han, Z. Li, T. T. B. Tram, K. S. Sim, C. M. Parry, N. T. Chinh,
493 H. Vinh, N. P. H. Lan, N. T. V. Thieu, P. V. Vinh, S. Koirala, S. Dongol, A. Arjyal, A. Karkey,
494 O. Shilpakar, C. Dolecek, J. N. Foo, L. T. Phuong, M. N. Lanh, T. Do, T. Aung, D. N. Hon,
495 Y. Y. Teo, M. L. Hibberd, K. L. Anders, Y. Okada, S. Raychaudhuri, C. P. Simmons, S.
496 Baker, P. I. W. de Bakker, B. Basnyat, T. T. Hien, J. J. Farrar, C. C. Khor, Variation at HLA-
497 DRB1 is associated with resistance to enteric fever. *Nat. Genet.* **46**, 1333–1336 (2014).

498 59. C. C. Chang, C. C. Chow, L. C. Tellier, S. Vattikuti, S. M. Purcell, J. J. Lee, Second-
499 generation PLINK: rising to the challenge of larger and richer datasets. *Gigascience*. **4**, 7
500 (2015).

501 60. J. H. Hankin, D. O. Stram, K. Arakawa, S. Park, S. H. Low, H. P. Lee, M. C. Yu, Singapore
502 Chinese Health Study: development, validation, and calibration of the quantitative food
503 frequency questionnaire. *Nutr. Cancer*. **39**, 187–195 (2001).

504 61. R. Dorajoo, X. Chang, R. L. Gurung, Z. Li, L. Wang, R. Wang, K. B. Beckman, J. Adams-
505 Haduch, Y. M, S. Liu, W. Y. Meah, K. S. Sim, S. C. Lim, Y. Friedlander, J. Liu, R. M. van
506 Dam, J.-M. Yuan, W.-P. Koh, C. C. Khor, C.-K. Heng, Loci for human leukocyte telomere
507 length in the Singaporean Chinese population and trans-ethnic genetic studies. *Nat.*
508 *Commun.* **10**, 2491 (2019).

509 62. X. Chang, R. L. Gurung, L. Wang, A. Jin, Z. Li, R. Wang, K. B. Beckman, J. Adams-
510 Haduch, W. Y. Meah, K. S. Sim, W. K. Lim, S. Davila, P. Tan, J. X. Teo, K. K. Yeo, Y. M, S.
511 Liu, S. C. Lim, J. Liu, R. M. van Dam, Y. Friedlander, W.-P. Koh, J.-M. Yuan, C. C. Khor,
512 C.-K. Heng, R. Dorajoo, Low frequency variants associated with leukocyte telomere length
513 in the Singapore Chinese population. *Commun Biol*. **4**, 519 (2021).

514 63. X. Chang, R. Dorajoo, Y. Sun, L. Wang, C. N. Ong, J. Liu, C. C. Khor, J.-M. Yuan, W. P.
515 Koh, Y. Friedlander, C.-K. Heng, Effect of plasma polyunsaturated fatty acid levels on
516 leukocyte telomere lengths in the Singaporean Chinese population. *Nutr. J.* **19**, 119 (2020).

517 64. X. Chang, R. Dorajoo, Y. Sun, Y. Han, L. Wang, C.-C. Khor, X. Sim, E.-S. Tai, J. Liu, J.-M.
518 Yuan, W.-P. Koh, R. M. van Dam, Y. Friedlander, C.-K. Heng, Gene-diet interaction effects
519 on BMI levels in the Singapore Chinese population. *Nutr. J.* **17**, 31 (2018).

520 65. X. Chang, A. Salim, R. Dorajoo, Y. Han, C.-C. Khor, R. M. van Dam, J.-M. Yuan, W.-P.
521 Koh, J. Liu, D. Y. Goh, X. Wang, Y.-Y. Teo, Y. Friedlander, C.-K. Heng, Utility of genetic
522 and non-genetic risk factors in predicting coronary heart disease in Singaporean Chinese.
523 *Eur. J. Prev. Cardiol.* **24**, 153–160 (2017).

524 66. H. Li, C. B. E. Chee, T. Geng, A. Pan, W. P. Koh, Joint Associations of Multiple Lifestyle
525 Factors With Risk of Active Tuberculosis in the Population: The Singapore Chinese Health
526 Study. *Clin. Infect. Dis.* **75**, 213–220 (2022).

Acknowledgements: We thank Angus Y. Lee and Harmandeep S. Dhaliwal (UC Berkeley Cancer Research Laboratory) for generation of *Aldh2* mutant mice. We thank all the participants involved in the genetics studies in Vietnam and Singapore. We acknowledge the clinical and laboratory staff at the study sites in Vietnam and Singapore for their contribution, especially Phan Vuong Khac Thai, Maxine Caws, Nguyen Duc Bang, Tran Thi Hong Chau, Guy Thwaites, and their teams at Oxford University Clinical Research Unit, and Pham Ngoc Thach Hospital for TB and Lung Diseases, Ho Chi Minh City, Vietnam. We thank Zheng Li from the Genome Institute of Singapore for his contribute to the TB GWAS. We thank Karen Elkins for the gift of the Francisella LVS strain as well as helpful advice and protocols. **Funding:** We thank the NIH for the following support: ES 28096 (C.J.C.), AI066302 (R.E.V., S.A.S.), AI153197 (S.A.S., K.H.D.). C.J.C. is a CIFAR Fellow. R.E.V. is an Investigator of the Howard Hughes Medical Institute. The Vietnam human genetics work was supported by the National Health and Medical Research Council Australia: 1056689 (SJD) and 1172853 (SJD). The Singapore Chinese Health Study was supported by grants from the National Medical Research Council, Singapore (NMRC/CIRG/1456/2016), National Institutes of Health (R01 CA144034 and UM1 CA182876) and National Research Foundation, Singapore (Project Number 370062002). **Author contributions:** Conceptualization: HD, SAS; Data Curation: SAS, HD, SB; Formal analysis: SB, XC, DK, DF, SAS; Investigation: SB, SE, DF, AAS, LT; Resources: NTTT, RD, CCK, CKH, JMY; Supervison: RV, SD, SAS, HD; Writing: SAS, SD; Review and Editing: all authors. **Competing interests:** S.A.S. is on the SAB for X-biotix Therapeutics. R.E.V. is on the SAB for Tempest Therapeutics and X-biotix Therapeutics. **Data and materials availability:** all data is available in the manuscript with the exception of the scRNAseq data which has been deposited in GEO.

List of Supplementary Materials

Materials and Methods

Figs. S1 and S2

Materials and Methods

Ethics Statement:

All procedures involving the use of mice were approved by the University of California (UC) Berkeley, Institutional Animal Care and Use Committee (Protocol #2015-09-7979-1). All protocols conform to federal regulations, the National Research Council Guide for the Care and Use of Laboratory Animals, and the Public Health Service Policy on Humane Care and Use of Laboratory Animals. All experiments handling *M. tuberculosis* were conducted in Biosafety Level 3 facilities in accordance with Environmental Health and Safety guidelines, and all experiments handling *F. tularensis* LVS were conducted in Biosafety Level 2 facilities. All study protocols for PTB and TBM human studies were approved by the Institutional Review Boards of Pham Ngoc Thach Hospital for TB and Lung Disease and The Hospital for Tropical Diseases Ho Chi Minh City (HCMC), Vietnam, HCMC Health Services, Vietnam and the Oxford Tropical Research Ethics Committee, UK. Approval for the genetics study was also granted from the Health Sciences Human Ethics Sub-Committee at the University of Melbourne, Australia (ID: 1340458). Written informed consent was obtained from all participants. All studies in SCHS were approved by the Institutional Review Board at National University of Singapore, and written informed consent was obtained from all participants.

Mice:

C57BL/6J (#000664) mice were obtained from The Jackson Laboratory (Bar Harbor, ME) and bred in-house. *Sp140*$^{-/-}$ mice were generated previously (*29*) and bred in-house. *Aldh2*$^{-/-}$ mice were generated in the process of recapitulating the human *ALDH2*2* mutation in *Sp140*$^{-/-}$ mice. *Aldh2*2 Sp140*$^{-/-}$ mice were generated by pronuclear injection of Cas9 mRNA, sgRNA, and a 154 nucleotide ultramer oligo (IDT Inc., Coralville, IA) containing 77 and 39 nucleotide homology arms and encoding the *Aldh2*2* mutation as well as synonymous mutations that disrupt sgRNA binding, as previously described (*46*). Founder mice were genotyped for *Aldh2*2* mutations by PCR using the forward primer 5' GGAGAGGTGTGCTGTGTT 3' and the reverse primer 5' GGGATCTGTATTCCGTGGC 3' and then sequencing using the same forward primer. Founders carrying the *Aldh2*2* mutation or deletions in *Aldh2* (i.e., *Aldh2*$^{-/-}$) were bred one generation to *Sp140*$^{-/-}$ mice to separate modified *Aldh2* haplotypes. Resulting pups with matched *Aldh2* haplotypes were interbred to generate homozygous lines that were maintained in-house.

Bacterial Culture:

Frozen stocks of low passage *M. tuberculosis* H37Rv, *M. tuberculosis* Erdman, and *M. tuberculosis* Lux-Erdman (a reporter strain that constitutively expresses the bacterial luciferase encoding luxCDABE operon, gift from Cox Laboratory at UC Berkeley) were grown to logarithmic phase over 4-5 days at 37°C in Middlebrook 7H9 media with 10% albumin-dextrose-saline, 0.5% glycerol, and 0.05% Tween-80 ("7H9c"). For preparation of aerosol stocks of *M. tuberculosis* H37Rv and Erdman, logarithmic phase cultures were centrifuged at 3,500 rpm for 5 min., resuspended in 1X phosphate-buffered saline (PBS), and sonicated thrice for 30 sec. each at 90% power. Cultures were then centrifuged at 700 rpm for 5 min to pellet large clumps, the supernatant was collected, and then centrifuged again at 700 rpm for 5 min. The supernatant was then collected and the OD600 was measured to determine bacterial concentration, and then aliquoted and frozen at -80°C until use. Frozen stocks of *Francisella tularensis* live vaccine

598 strain (LVS) (generously gifted by Dr. Karen Elkins, FDA) was cultured in Muller Hinton Broth
599 containing 1.25 mM $CaCl_2$, 2.2 mM $MgCl_2$, 0.1% glucose, 0.025% ferric pyrophosphate, and 2%
600 Isovitalex (#211875, Becton Dickinson, Franklin Lakes, NJ) to early log phase (OD600 ≈ 0.25)
601 overnight for use in experiments. For preparation of injection stocks of *F. tularensis* LVS, frozen
602 stocks were thawed at room temperature and then diluted in sterile 1X PBS to the desired
603 concentration.
604
605 *In Vitro Macrophage Isolation and Culture:*
606 Bone-marrow was obtained from *Aldh2*$^{-/-}$, *Aldh2*$^{-/-}$*Sp140*$^{-/-}$, *Sp140*$^{-/-}$, and C57BL/6J (B6) mice
607 and cultured in DMEM (#11960-044, Thermo Fischer Scientific, Waltham, MA) containing 10%
608 FBS, 2 mM L-glutamine, and 10% supernatant from 3T3-M-CSF cells (BMDM media) for 6 days
609 with media supplementation on day 3 to generate bone marrow-derived macrophages
610 (BMDMs). BMDMs were then harvested and frozen in liquid nitrogen in 40% FBS, 10% DMSO,
611 and 50% BMDM media until use.
612
613 *In Vitro Macrophage Stimulation:*
614 BMDMs were plated in 96-well plates at $5x10^4$ cells/well and allowed to adhere for 48 hours
615 prior to analysis. 24 hours prior to analysis, BMDMs were stimulated with IFNγ (≈ 30 ng/mL) and
616 PAM3CSK4 (50 ng/mL). BMDM aldehyde levels were quantified using Mito-RFAP-2, a
617 mitochondrial-target version of ratiometric formaldehyde dye RFAP-2 (*47*, *48*). Briefly, Mito-
618 RFAP-2 was dissolved in DMSO to a concentration of 10 mM and diluted to 10 μM in Hank's
619 Balanced Salt Solution (HBSS); the probe was then added to the BMDMs for 30 min. at
620 37°C/5% CO_2. BMDMs were then rinsed once with HBSS to remove the probe and allowed to
621 incubate in BMDM media for 60 min. at 37°C/5% CO_2. The cells were then analyzed by
622 fluorescent excitation at 405 nm and 488 nm and emission at 510 nm. Fluorescence was
623 measured using a SpectraMax M3 plate reader (Molecular Devices, San Jose, CA) and
624 reported as the ratiometric value of emission at 405 nm and 488 nm excitations.
625
626 *In Vitro Macrophage Infections:*
627 For infection with *M. tuberculosis*, BMDMs were plated in 96-well plates at $5x10^4$ cells/well and
628 allowed to adhere for 48 hours prior to infection. 24 hours prior to infection, media was changed
629 and BMDMs were stimulated with IFNγ (≈ 30 ng/mL) for IFNγ+ conditions. 5 days prior to
630 infection, a frozen stock of *M. tuberculosis* Lux-Erd was thawed and cultured in 7H9 at 37°C to
631 log phase (OD600 = 0.2 – 1.0). *M. tuberculosis* was centrifuged at 3500 rpm for 5 min. and
632 washed twice in PBS, centrifuged at 500 rpm for 5 min. to pellet clumps, and then sonicated at
633 90% power (twice, 30 sec. each). After sonication, cultures were diluted in DMEM + 5% horse
634 serum + 5% FBS and added to the BMDMs at a multiplicity of infection (MOI) of 1, followed by
635 spinfection at 1200 rpm for 10 min. Supernatant was then removed and the infected BMDMs
636 were washed twice with 1X PBS before the appropriate media was added and the cells were
637 incubated at 37°C/5% CO_2 until the first time point. CFU were enumerated at the indicated time
638 points by washing infected cells twice with PBS, lysing in sterile-filtered deionized water with
639 0.5% Triton X-100 for 10 min. at 37°C/5% CO_2, and performing serial dilutions in 1X PBS
640 containing 0.05% Tween 80 before aliquoting dilutions onto Middlebrook 7H10 plates
641 supplemented with 0.5% glycerol and 10% OADC (Middlebrook) and incubated for 21 days at

642 37°C. CFU is normalized to inoculum dose, calculated by plating t = 0 CFU immediately after
643 spinfection. For infection with *F. tularensis* LVS, BMDMs were prepared as described above.
644 BMDMs were plated in a 24-well plate at $3x10^5$ cells/well and allowed to adhere for 48 hours
645 prior to infection. 24 hours prior to infection, media was changed and BMDMs were stimulated
646 with IFNγ (≈ 30 ng/mL) for IFNγ+ conditions. To infect the BMDMs, *F. tularensis* LVS stocks
647 were thawed, resuspended in BMDM media, and added to the BMDMs at an MOI = 0.1 and
648 allowed to phagocytose for 2 hours at 37°C/5% CO_2. After phagocytosis, infected BMDMs were
649 washed thrice with 1X PBS and then supplemented with normal media until predetermined time
650 points. To enumerate CFU/well, BMDMs were rinsed once with 1X PBS, lysed with sterile-
651 filtered deionized water for 10 min., and then serial dilutions were plated on Mueller Hinton
652 plates containing 85 mM NaCl, 1% (w/v) proteose peptone/tryptone, 8% (w/v) bacto-agar, 0.1%
653 glucose, 0.025% ferric pyrophosphate, 2% Isovitalex, and 2.5% bovine serum for 3 days at
654 37°C/5% CO_2 until CFU were counted.
655
656 *Immunoblotting:*
657 BMDMs were prepared as previously described and plated in a 24-well plate at $3x10^5$ cells/well,
658 and infected with *M. tuberculosis* H37Rv according to the previously described protocol. 24
659 hours post infection, BMDMs were rinsed with 1X PBS and lysed with Laemmli Buffer
660 (#1610737EDU, Bio Rad, Hercules, CA). Samples were heat inactivated/sterilized at 100°C for
661 20 min. prior to removal from the BSL3 facility. Protein lysates were prepared by heating in 1X
662 SDS for 5 min. at 100°C and then analyzed by SDS-PAGE using 4-20% Criterion TGX Precast
663 Protein Gel (#5678094, Bio Rad), rabbit monoclonal antibody (EPR4494) against ALDH2
664 (#ab133306, Abcam, Cambridge, MA), and an anti-rabbit HRP-conjugated secondary antibody.
665 Blots were developed with Western Lightning Plus-ECL enhanced chemiluminescence
666 substrate (#NEL103001EA, PerkinElmer, Waltham, MA) and a ChemiDoc MP/475D Imaging
667 System (Bio Rad).
668
669 *Single Cell RNAseq:*
670 Single cell RNA sequencing results were extracted from a previously published dataset (*49*) on
671 *M. tuberculosis*-infected B6 mice. For bulk RNAseq, BMDMs were prepared as previously
672 described and plated in a 24-well plate at $3x10^5$ cells/well, and infected with *M. tuberculosis*
673 H37Rv according to the previously described protocol. 24 hours post infection, BMDMs media
674 was removed and cells were lysed with TRIzol Reagent (#15596018, Thermo Fisher Scientific).
675 RNA was extraction was performed by adding chloroform and centrifuging samples to make a
676 biphasic mixture containing RNA in an aqueous phase. The RNA-containing phase was then
677 collected and cleaned up using a RNeasy Mini Kit (#74104, Qiagen, Hilden, Germany) with on-
678 column DNase digestion according to the manufacturer's protocol. The isolated RNA was then
679 quantified and analyzed by a Qubit Quantitation Platform and an Agilent 2100 Bioanalyzer,
680 respectively, at the Functional Genomics Laboratory of the California Institute for Quantitative
681 Biosciences (UC Berkeley), and then submitted to GeneWiz/Azenta Life Sciences (South
682 Plainfield, NJ) for library preparation and sequencing. Each sample was dual-indexed using
683 NEBNext multiplex oligomers and then quantity and quality were assessed with a Qubit Broad
684 Range Kit and bioanalyzer, respectively. All samples had a RIN > 9.8 and 100 ng of total RNA
685 was used in library preparation. Samples were then prepared for sequencing using a NEBNext

686 Ultra II RNA-seq with Poly-A selection kit, and sequenced on a NovaSeq 6000 S4 (partial lane),
687 with a sequencing depth of 29 million paired-end reads per sample. Illumina sequencing data
688 files were pre-processed with HTStream (v. 1.3.0) to remove PCR duplicates, trim adapters,
689 polyA tails, and N characters, and to remove low quality 3' and 5' bases (*50*), and were checked
690 for quality with FastQC (v. 0.11.7). Sequences were aligned to the mouse primary assembly
691 GRCm39 from GENCODE (*51*) and gene counts were generated using STAR (v.
692 2.7.10b_alpha_230301 (*52*)). RNAseq data is submitted
693
694 *Aldehyde susceptibility assays:*
695 *M. tuberculosis* H37Rv was cultured as described above. To test susceptibility to various
696 aldehydes, cultures were grown to an optical density at 580 nm (OD_{580}) of 0.8-1.0. Bacteria
697 were collected by centrifugation at 3,200 *g* and resuspended in 7H9c acidified to pH 5.5 with 1N
698 HCl and clumped cells were removed with a slow-speed spin at 150 *g*. The supernatant was
699 diluted to an OD_{580} of 0.08. 200 µl of bacteria was added to wells of a 96-well plate; for each
700 condition tested, three wells were prepared. Two µL of 1:100 aldehyde stock solutions were
701 added to each well to obtain the final concentrations indicated in the Figure 2 (A-C). Aldehydes
702 were purchased from the following: 4-hydroxynonenal (4HNE) (# 32100, Cayman Chemical,
703 Ann Arbor, MI), malondialdehyde (MDA) (#63287, Millipore Sigma, Burlington, MA), and
704 formaldehyde (FA) (#15710, Electron Microscopy Sciences, Hatfield, PA) (16%
705 paraformaldehyde solution, stored in aliquots at -20˚C). To generate nitric oxide (NO), sodium
706 nitrite was added to a final concentration of 3 mM. To test the susceptibility of *F. tularensis* LVS
707 to various aldehydes, we followed a previously described protocol (*30*). Briefly, *F. tularensis*
708 LVS was plated on Mueller Hinton plates for 3 days at 37°C/5% CO_2. Multiple colonies colony
709 were then scraped and used to inoculate a liquid culture (to ensure diversity of the culture) that
710 was maintained at 37°C/180 rpm for 12-14 hours. The culture was then washed twice in 1X PBS
711 and resuspended at an OD600 = 0.01 in 1X PBS and aliquoted into a 96-well plate containing
712 various concentrations of 4HNE (#32100, Cayman Chemical Company), MDA (#63287,
713 Millipore Sigma), or FA (#F1635, Millipore Sigma) and incubated for 2 hours at 37°C/5% CO_2.
714 After incubation, CFU/well was enumerated for each condition by plating serial dilutions of the
715 culture on Mueller Hinton plates and incubating at 37°C/5% CO_2 for 3 days.
716
717 *In Vivo Pathogen Challenge:*
718 Mice were infected with *M. tuberculosis* H37Rv (*Aldh2*$^{-/-}$ and B6 mice), or *M. tuberculosis*
719 Erdman (*Aldh2*$^{-/-}$ and *Aldh2*$^{-/-}$ *Sp140*$^{-/-}$ mice) *via* the aerosol route. Aerosol infection was
720 performed using a nebulizer and full-body inhalation exposure system (Glas-Col, Terre Haute,
721 IN). Previously prepared aerosol stocks were thawed and 9 mL of culture diluted into sterile-
722 filtered deionized water was loaded into the nebulizer calibrated to deliver ~25 CFU/mouse, as
723 measured by CFU in the lungs 1 day following infection (data not shown). At predetermined time
724 points, mice were euthanized and the lungs were mechanically homogenized in 1X PBS
725 containing 0.05% Tween 80 and serial dilutions were plated on 7H10 plates and incubated for
726 21 days at 37°C until CFU were counted. For mice infected with *F. tularensis* LVS, injection
727 stocks were prepared as previously described and ~10^6 CFU were administered intradermally
728 into the rump of the mouse, as measured by plating serial dilutions of the inoculum on Mueller
729 Hinton plates (data not shown). At 5 dpi, mice were euthanized and the lungs were

730 mechanically homogenized in 1X PBS and serial dilutions were plated on Mueller Hinton plates
731 and incubated for 3 days at 37°C/5% CO_2 until CFU were counted.
732
733 *Candidate Gene Analysis Study:*
734 Study subjects from the Vietnam human genetics collection have been described in detail
735 previously (*53*). The TB participants were recruited at several clinical sites in Ho Chi Minh City,
736 Vietnam as part of larger clinical studies with strictly defined clinical phenotypes (*54–56*). The
737 Vietnamese population controls are otherwise healthy adults with primary angle closure
738 glaucoma who have been previously described (*57*). DNA from all participants were genome
739 wide genotyped on the Illumina Omni Express array v1.0 and standard quality control measures
740 and pipelines were applied as described previously (*57*, *58*). In order to examine the association
741 between rs671 and TB, we extracted genotypes for rs671 from the genotyping data generated
742 for the genome-wide association study (GWAS). Logistic regression was applied with
743 adjustment for the first three principal components (PCs) to control any potential population
744 structure. The analysis was done for all TB cases first. Similar analysis was repeated for clinical
745 phenotypes. All analyses were carried out using Plink 1.9 (www.cog-
746 genomics.org/plink/1.9/)(*59*).
747
748 SCHS is a long-term prospective population-based cohort study focused on genetic and
749 environmental determinants of cancer and other diseases in Singapore (*60*). From April 1993 to
750 December 1998, the study recruited 63,257 participants of Singaporean Chinese descent,
751 hailing from the Hokkien and Cantonese dialect groups. Starting from April 1994, a random
752 subset of 3% of participants were invited to contribute blood/buccal cell and spot urine samples.
753 In January 2001, the collection of biospecimens was expanded to include all enrolled
754 participants who provided consent and approximately half of all study participants donated blood
755 or buccal samples for genetic studies. A total of 27,308 samples were whole genome genotyped
756 using the Illumina Global Screening Array (GSA). Comprehensive information regarding
757 genotyping and QC protocols has been previously published (*61*, *62*). Genotype data for rs671
758 was extracted from the GSA array data for subsequent statistical analysis. Additional 2,003
759 independent subjects from the SCHS CAD-nested case-control study were genotyped on the
760 Illumina HumanOmniZhonghua Bead Chip. GWAS genotyping and QC procedures for this
761 dataset has been extensively described (*63–65*). Genotype data for rs671 after 1000 Genomes
762 imputation procedures were extracted from the SCHS CAD dataset for statistical analysis.
763 Active TB cases in the SCHS were identified through linkage of the cohort database with the
764 National TB Notification Registry until 31 December 2016 (*66*). The association between rs671
765 and active PTB status was assessed via logistic regression with adjustment for age and gender.
766 Subsequently, fixed-effect inverse-variance weighted (IVW) method was employed for meta-
767 analysis of the results from Vietnam and Singapore. Cochran's Q ($P_{Het} < 0.05$) were evaluated
768 as an indication of heterogeneity. All analysis was conducted using Stata/SE15.1.
769
770 *Statistical Analysis:*
771 Data are presented as mean values and error bars represent standard deviation. The number of
772 samples, experimental replicates, and statistical tests are described in the legend of each figure.
773 Statistical analyses were performed using GraphPad Prism 9 (GraphPad, La Jolla, CA) and a p
774 < 0.05 was considered significant.
775

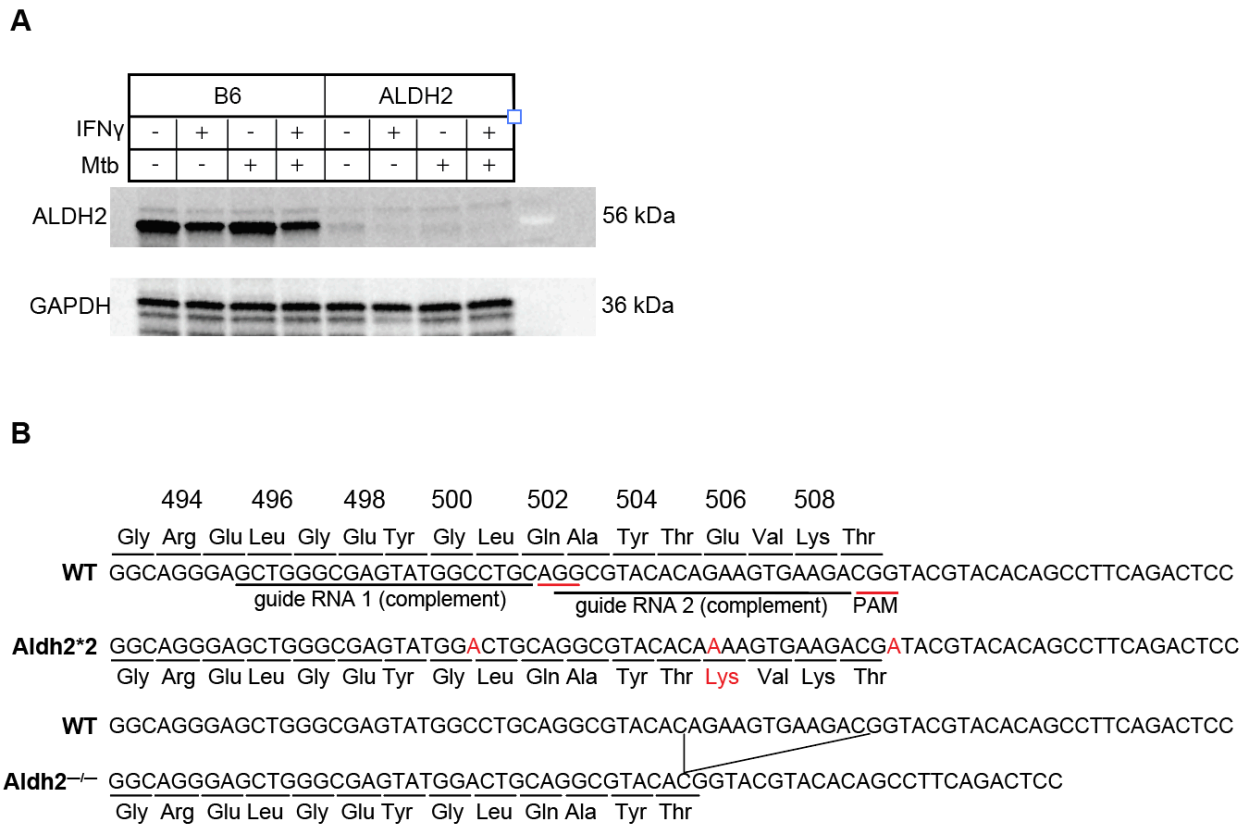

Figure S1. Genetic knock out of *Aldh2* inhibits ALDH2 production. A) Immunoblot of WT and *Aldh2*$^{-/-}$ BMDM cell lysates stained with αALDH2 (56 kDa) and αGAPDH (36 kDa, control). B) CRISPR targeting strategy of *Aldh2*2* mice, resulting in mutants containing three adenine point mutations (first and third adenines disrupt sgRNA binding, while second adenine is the human mutation) (*Aldh2*2* mice) and mice containing a 12 bp (4 amino acid) in-frame deletion (*Aldh2*$^{-/-}$ mice).

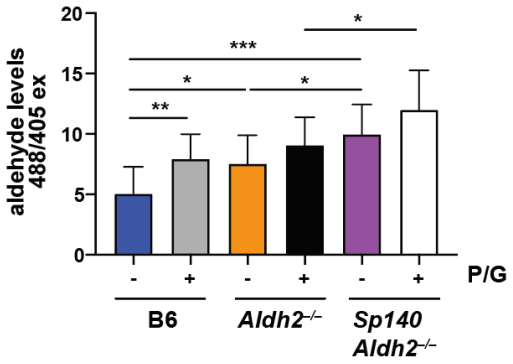

Figure S2. *Sp140*$^{-/-}$*Aldh2*$^{-/-}$ demonstrate increased mitochondrial aldehyde levels. A) WT, *Aldh2*$^{-/-}$, and *Sp140*$^{-/-}$*Aldh2*$^{-/-}$ BMDM mitochondrial-associated formaldehyde levels after 24 hours stimulation with IFNγ and TLR2-agonist PAM3CSK4 *in vitro* (n = 3 independent experiments, B6 and *Aldh2*$^{-/-}$ results are same as reported in Fig. 3A). *, $p < 0.05$, **, $p < 0.01$, ***, $p < 0.001$, Unpaired t-test.